## Regular paper

# A sub-glacial sediment deformation model from geotechnical and structural properties of an overconsolidated lacustro-glacial clay

F. Schokking

Geological Survey of The Netherlands, P.O. Box 157, 2000 AD Haarlem, The Netherlands

Received 13 September 1988; accepted in revised form 30 November 1989

Key words: engineering geology, geotechnical properties, sub-glacial sediment deformation, lacustro-glacial clay, overconsolidation

#### **Abstract**

Sub-glacial deformation processes of ice sheets are recorded in geotechnical and structural properties of overriden sediments.

Geotechnical, structural and microstructural properties were determined of Late-Pleistocene lacustroglacial clays in the northern Netherlands that were subjected to deformation by the Saalian ice sheet. From these properties a sub-glacial deformation model could be constructed of the clay sequence, depicting an extensively sheared upper zone and a lower zone that was folded, hydrodynamically consolidated and fissured during subsequent phases of ice sheet development.

This sub-glacial deformation model can serve as a basis for a model of the distribution of geotechnical properties of the clays which has applications in engineering geology and geotechnical engineering.

#### Introduction

The lacustro-glacial 'Pot Clay' of the Peelo Formation, which was laid down during the Elsterian glaciation of the Late-Pleistocene, is known to be overconsolidated by the load of an ice sheet, during the Saalian glaciation.

Site investigations carried out for civil engineering constructions revealed changes with depth in the strength and overconsolidation ratio of the clays (Schokking 1984). Since as yet poorly understood sub-glacial deformation processes were suspected to have caused a particular distribution of geotechnical properties, a borehole was drilled near Marum, Province of Groningen (Fig. 1), to investigate these phenomena.

Thirty three undisturbed open tube samples were taken continuously over the entire depth (approximately 40 m) of the  $250 \text{ mm} \varnothing$  cased shell and

auger borehole. The 100 mm Ø PVC sample tubes were placed within a conventional steel sampler. In the laboratory seventeen of the samples were lengthwise split in halves. Geotechnical index tests such as for natural water content, unit weight, plasticity, grain size distribution and undrained shear strength were performed, while the samples were also visually inspected and described. Oedometer consolidation tests were performed on nine samples taken at intervals throughout the depth of the borehole.

Observed deformation features and fissuring of the clay were also micromorphologically examined in thin sections and by Scanning Electron Microscope (SEM) imaging. For this purpose the Netherlands Soil Survey Institute at Wageningen made three large thin sections from two of the samples. The thin sections were prepared by the dry freezing method, followed by impregnation using Synolite 544 resin (Jongerius & Heintzberger 1975, Bisdom 1987).

The geotechnical and structural properties acquired allowed the construction of a sub-glacial deformation model. This model is important for glaciology, it also gives a better insight in the distribution of geotechnical properties in the Pot Clay.

# Geology

During and after the decay of the Elsterian ice sheet the lacustro-glacial Pot Clay was deposited, in glacial channels and basins that were formed in the northern Netherlands during the Elster glaciation (Ter Wee 1983b, Ehlers 1981). The channels, as present at Marum (Fig. 1 & 2), are more than approximately 5 km wide, more than 350 m deep and they generally trend north-south.

The lower parts of the channels and basins are filled with a fining upward sequence of mostly coarse granular sands and gravels. Locally, relatively thin silt and clay layers also occur.

Higher in the sequence, fine grained sands form the transition to the Pot Clay which caps the channels and basins. Fine granular sediments, also of the Peelo Formation, are often found flanking and on top of the Pot Clay.

The Pot Clay was possibly deposited after the channels were filled with coarser grained sediments to such a level, that a shallow basin with slowly flowing or stagnant water could develop that was dammed by melting and retreating ice.

Near Marum, but not at the location of the borehole, fine to medium coarse fluvial sands cover the Peelo sediments. These deposits belong to the Eindhoven Formation and are of Holsteinian age.

During the Saalian glaciation, a glacial till (Drente Formation) was deposited over the larger part of the area of the northern Netherlands. Erosion at the end of the Saalian and during the Weichselian, locally removed this till partly or entirely. During the Weichselian glaciation eolian cover sands and fluvio-periglacial deposits (Twente Formation) spread over the older deposits under periglacial conditions.

## Lithology of Marum borehole

In Fig. 3 the lithological sequence in the Marum borehole and the geophysical natural gamma and spontaneous potential logs are shown. In Figs 4 and 5 photographs of the halved tube samples are presented.

The top of the Pot Clay, immediately below the eolian cover sands and glacial till consists of an interlayering of sandy and clayey layers, ranging generally in thickness from 5 to 10 mm, but clay horizons up to 150 mm thick also occur. From approximately 10 m down to approximately 30 m, the clay is a rather homogeneous silty clay. Below that depth<sup>2</sup> the silt and sand content in the clay increases. Sand and clay layers are intermixed and thicknesses of individual layers vary from 5 to 500 mm. In Fig. 6 the variation in clay content (fraction  $< 2 \,\mu$ m) with depth is shown, which agrees well with the natural gamma log.

# A sub-glacial sediment deformation model

During the Saalian glaciation land ice reached from Scandinavia down to the central part of The Netherlands and covered the area of Marum. Apart from depositing a several metres thick glacial till in the northern part of the country, the ice considerably deformed the overridden sediments.

Granular soils were compacted by the weight of the ice to very high densities (Schokking 1985). In the central part of the Netherlands ice-pushed ridges and associated deep glacial basins were formed in granular soils near the ice sheet terminus (Van den Berg & Beets 1986).

Because of their ductile and plastic properties clays are even easier to deform. The Pot Clay sequence at Marum shows several deformation phenomena, which may be attributed to subsequent phases of the Saalian ice sheet development. The most important of these phenomena are shearing and folding, hydrodynamic consolidation and fissuring of the clays.

The geotechnical and structural properties which were determined on undisturbed samples in the

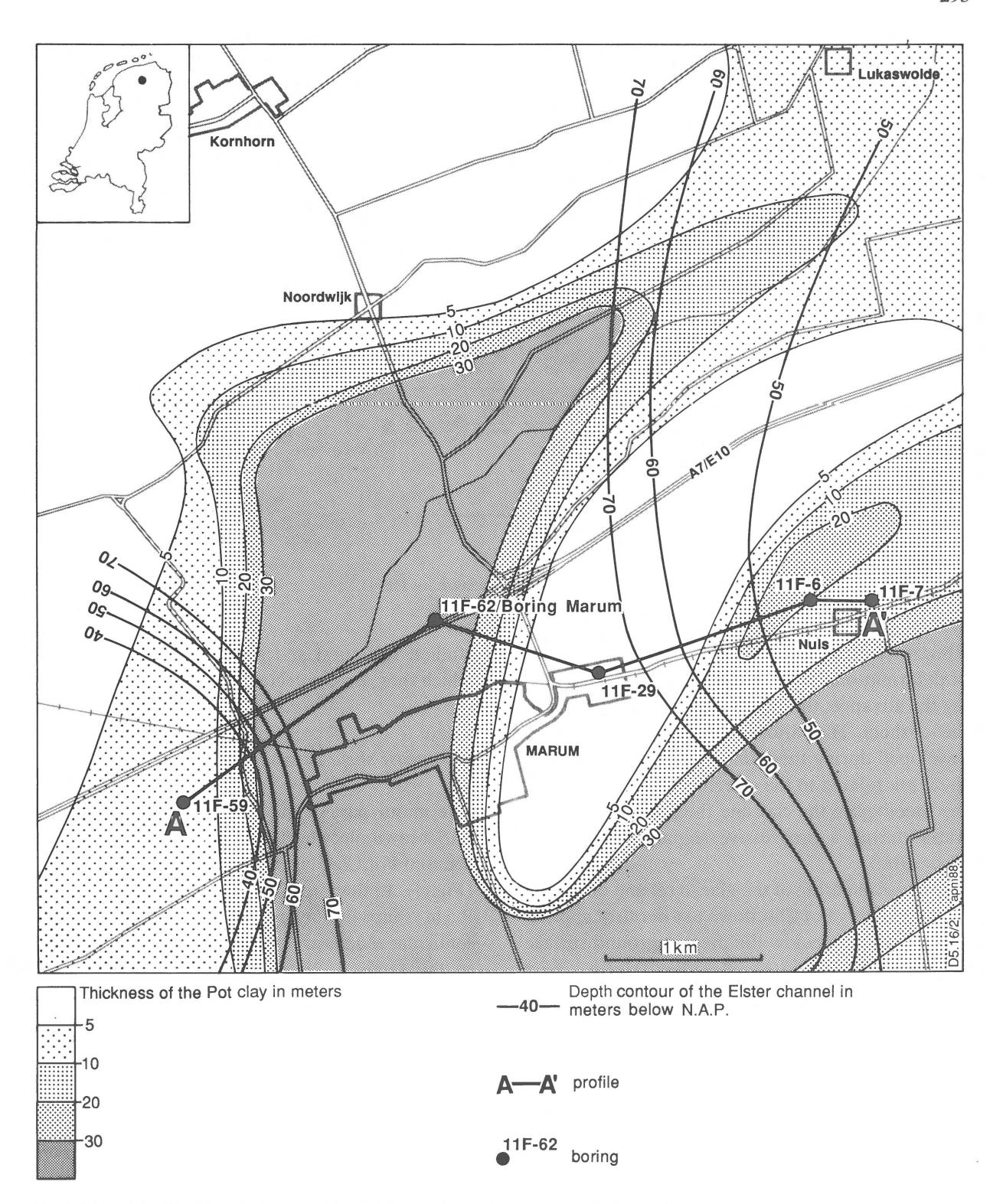


Fig. 1. Map of the Elsterian glacial channel near Marum. Inset: situation map of The Netherlands.

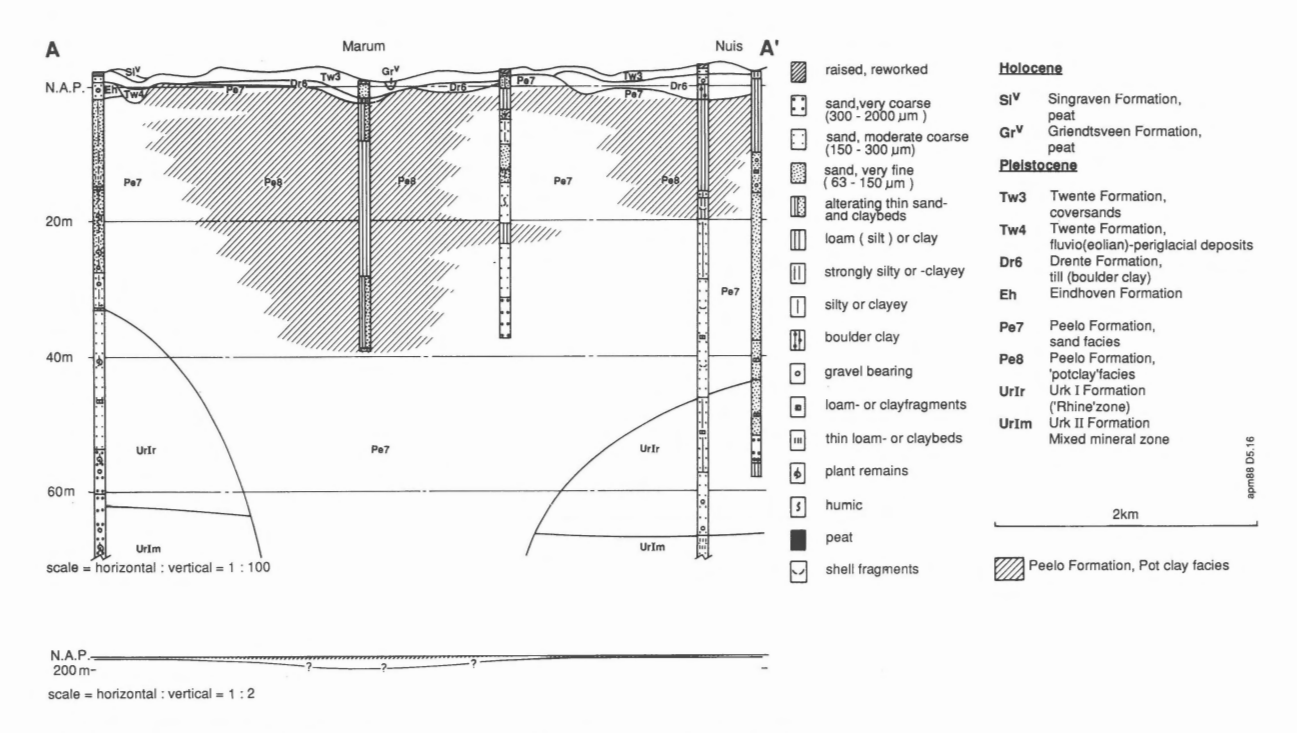


Fig. 2. Section through the Elsterian glacial channel near Marum (location see Fig. 1).

laboratory allow the construction of a simple model of deformational modes and processes acting during the advance, the steady state and the retreat of the ice sheet. The various types of deformation that developed during these different phases of the ice sheet are related to the effective stress conditions, the rheology of the clay and the phase of the pore water during a progressive sequence of events. These are:

- 1. Intense shearing of the glacial till and of the top of the sandy Pot Clay down to a depth of approximately 10 m below the present ground surface (Fig. 7).
- 2. Folding of Pot Clay, in a normally consolidated state, under frozen, partly frozen or unfrozen conditions, down to a depth of at least 30 m.
- Hydrodynamic consolidation of Pot Clay, increasing with depth under effective stress conditions up to 2100 kN/m<sup>2</sup>.
- 4. Fissuring of Pot Clay, below the base of the sandy Pot Clay, in an overconsolidated very stiff state.

In the next paragraphs these types of deformation will be further discussed and augmented with the studied structural and geotechnical properties to which they are connected.

### (1) Intense shear deformation

The major part of the glacial till is composed of dark brown silts which are mixed with black heavily sheared Pot Clay layers which are steeply inclined (Fig. 4). In the interval from approximately 3.5 to 9.5 m, thin sand layers occur in the Pot Clay and lenticular shapes are observed both in the clay and in the sand. As a result of the relatively small diameter of the samples, the lateral extent of these features cannot be established. They are interpreted as shear and boudinage structures.

The laboratory vane and fall cone values of  $s_u$  increase with depth from approximately  $50 \, kN/m^2$  at the top of the clay sequence, to between 150 and  $350 \, kN/m^2$  at  $10 \, m$  (Fig. 6). This has been observed in the Pot Clay in other locations as well. A comparison of laboratory test on samples from four different boreholes in an area between Marum and Delfzijl, at approximately  $50 \, km$  from Marum (Fig.

8), shows a steady increase of the undrained shear strength with depth in the Pot Clay, down to approximately 9 m. Below that depth the strength increases dramatically.

The natural water content as measured in the clay layers in between sand layers in the Marum borehole shows relatively high values, up to 40%. Below 10 m the natural water content decreases gradually with depth. In the studied area east of Marum similar features are observed (Fig. 8).

The estimated preconsolidation load, represent paleo-effective stresses (Fig. 9) and show much lower effective stresses in the upper part of the sequence than further down. Extrapolation of values to the upper zone indicates that effective stresses have ranged from 0 to  $500 \, kN/m^2$  within this zone.

Boulton & Hindmarsh (1987) propose a onedimensional sub-glacial deformation theory in which the empirical flow law is coupled to a model of sub-glacial hydrology and consolidation. They describe three possible states in which sub-glacial sediments can be in equilibrium. These are: stable states in which sediments do either not deform; a state in which a dilatant deforming horizon forms with positive effective pressures at the ice/sediment interface; and unstable states where zero or negative effective pressures are predicted. They define an upper, low density horizon, in which continuous deformation occurs in the whole sediment mass underlain by a horizon in which consolidation occurs and movements may take place along well defined planes.

The deforming zone described above, where the glacial till and a part of the sandy Pot Clay are intensely deformed, can be considered to be the upper low density horizon. In the Marum borehole this horizon had an original thickness of approximately 12 m before erosion of the glacial till. The lower boundary of the low density horizon is marked by a sudden increase in undrained shear strength  $s_u$ . Measurements from east of Marum show that regionally the depth of the low density horizon is about the same.

As infiltration of meltwater through the base of the low density horizon must be assumed to have been limited, the base of this horizon may have

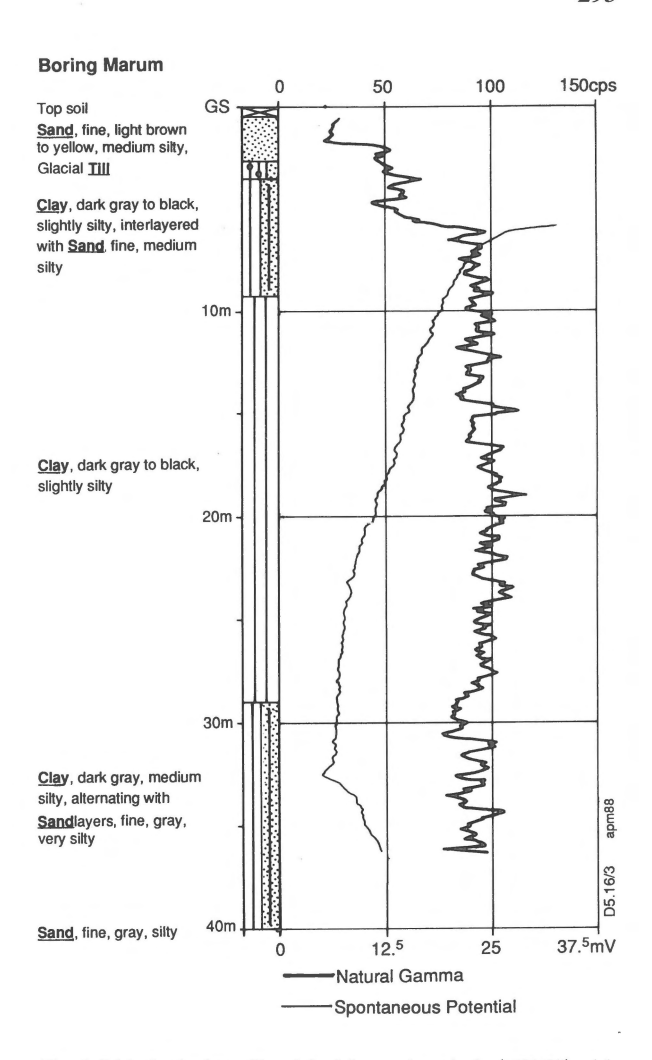
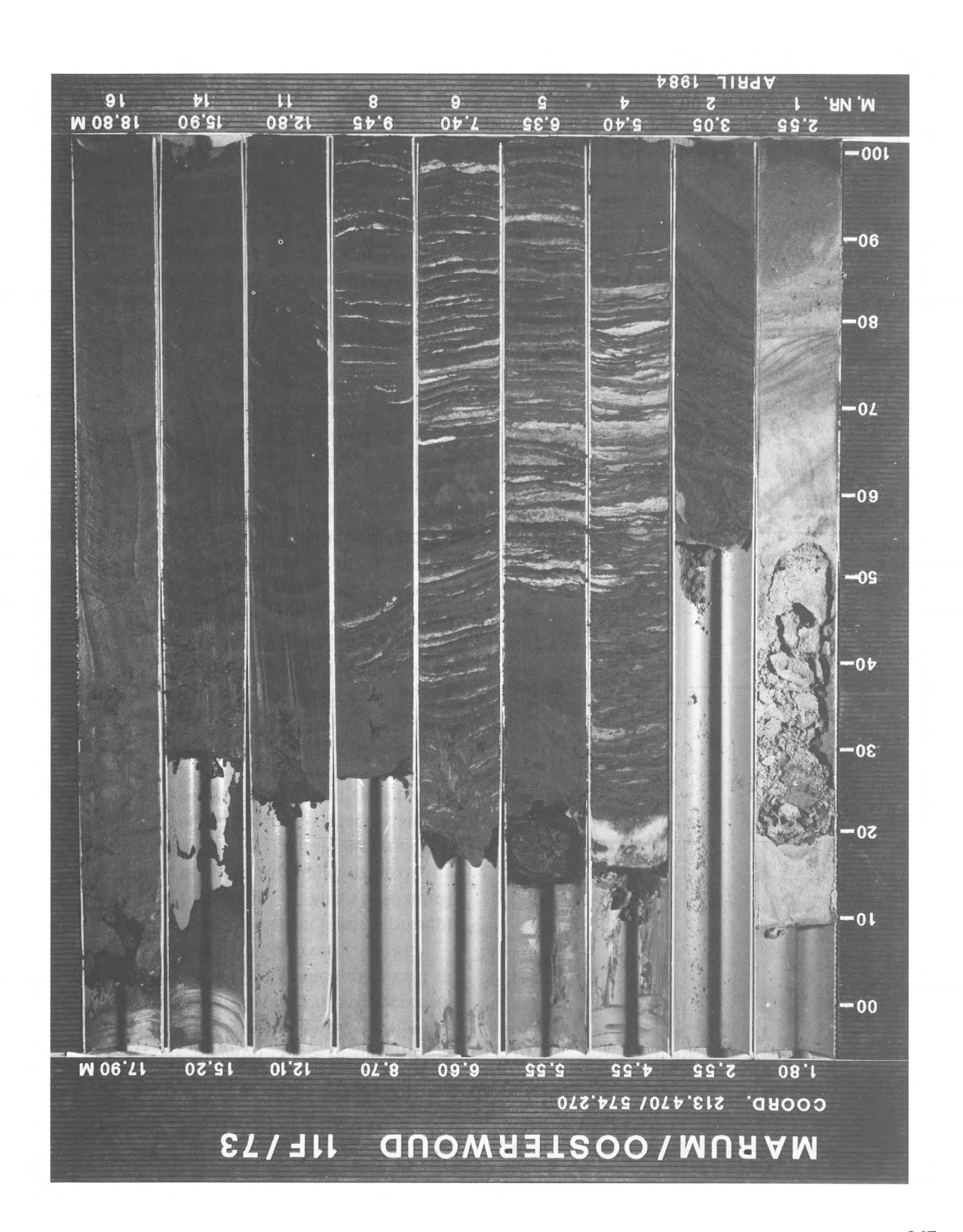
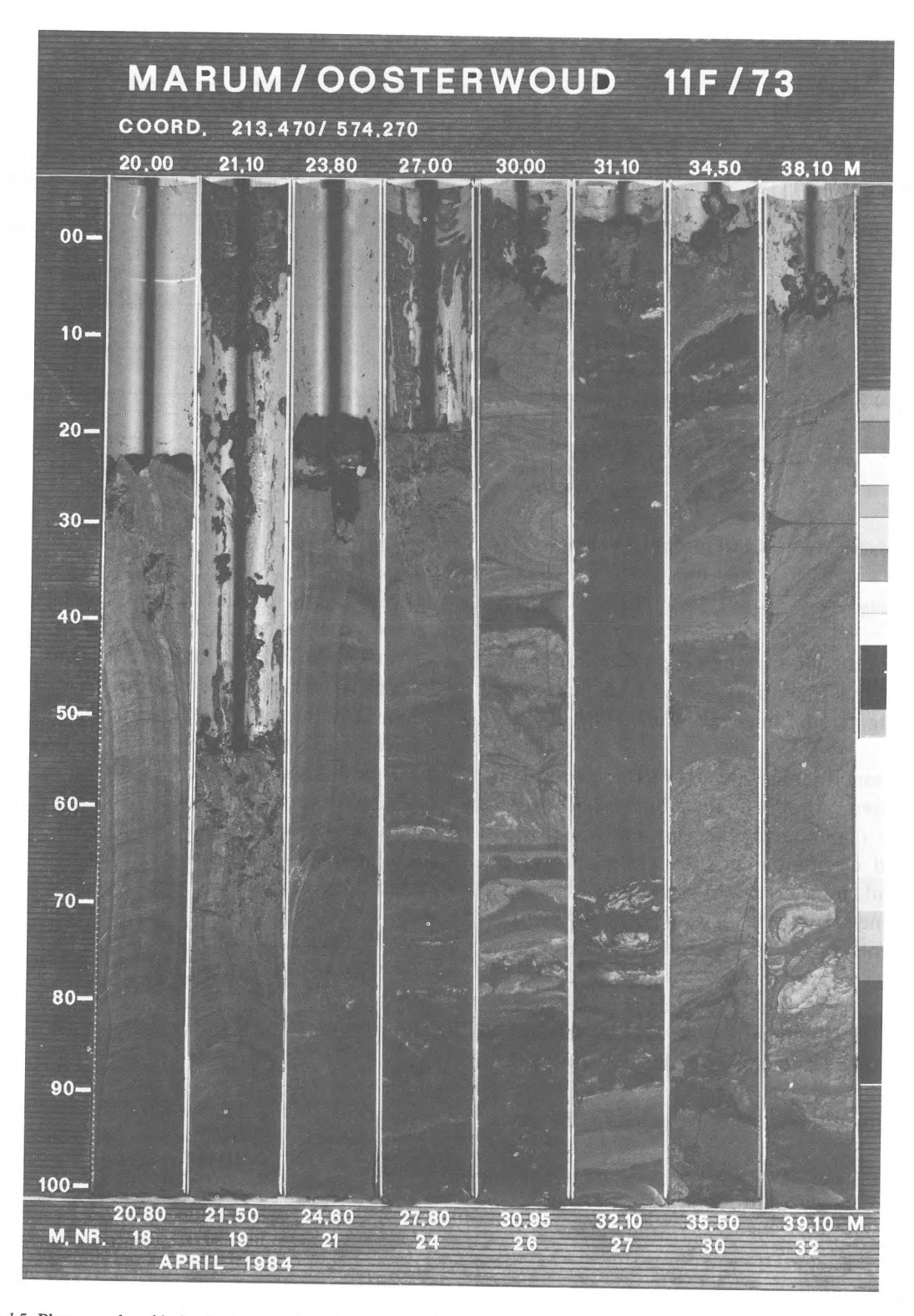


Fig. 3. Lithological profile of the Marum borehole (11F-73) with Natural Gamma and Spontaneous Potential logs.

been at a higher elevation in an early stage. Subsequently it moved down with decreasing permeability in the underlying horizon as a result of shearing and hydrodynamic consolidation in this horizon. The base of the low density horizon moved down until an effective stress level was reached, at which the clay strength was in equilibrium with the thrusting force of the ice.

Apart from periods during which temperatures in the sub-glacial sediments were below the pressure melting point, the low density horizon has been a zone with low effective stresses, low shear strength and strong deformation throughout the existence of the Saalian ice sheet.





Figs 4 and 5. Photographs of halved tube samples of the Marum borehole (11F-73).

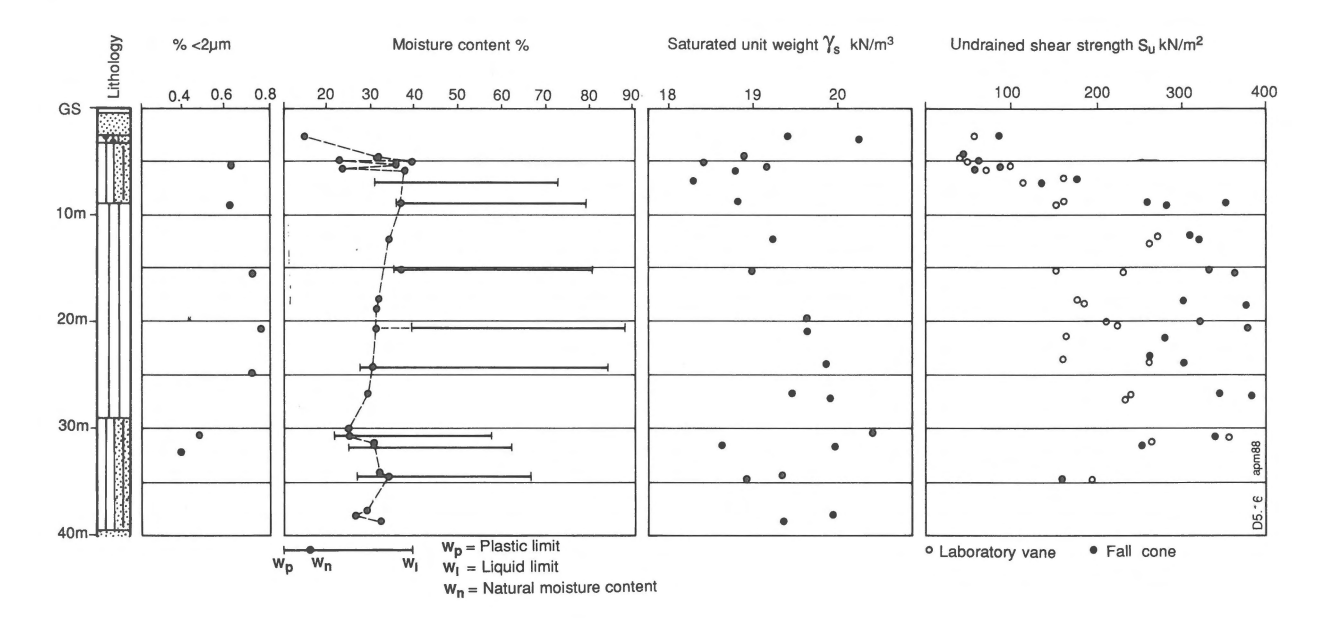


Fig. 6. Variation in geotechnical parameters with depth.

# (2) Folding

Folding of the Pot Clay in the zone underlying the low density horizon is observed both macroscopically (Fig. 5) and microscopically (Figs 10, 11 & 12).

In the sample from a depth of 29 m, microfolding was observed in very thin silt laminations (Figs 10 & 11). The diamond shaped clay particles, with a preferred orientation in the axial planes of the folds, and the segregation structures, also in the axial planes, are particularly noteworthy. This indicates folding of the clay in a frozen condition. The folds appear to have formed as a result of shearing along sub-horizontal axial planes.

Also, silt laminations have been observed that appear to be boudinaged, with thin clay layers in between.

Immediately after the ice advance the glacier sole can be expected to freeze onto the still frozen sediments causing folding with segregation features. Savigny & Morgenstern (1986) demonstrated in laboratory tests, that frozen clays can show creep behaviour at shear stress levels of 50 to  $100\,\mathrm{kN/m^2}$ , at temperatures of  $-2^\circ$  C. They did this in triaxial tests on frozen samples of clays, whose origin, composition and probable moisture content

were similar to those of the Pot Clay in its normally consolidated state. Recent observations at the base of the Urumqi Glacier in China indicate that frozen sub-glacial sediments deform much more readily than ice at the same temperature of  $-5^{\circ}$  C (Echelmeyer & Zhongxiang, 1987).

The observations described do not exclude that folding occurred under partly frozen or unfrozen ground conditions. Such folding would probably result particularly from shear during hydrodynamic consolidation (3).

#### (3) Hydrodynamic consolidation

Preconsolidation loads as determined in consoli-

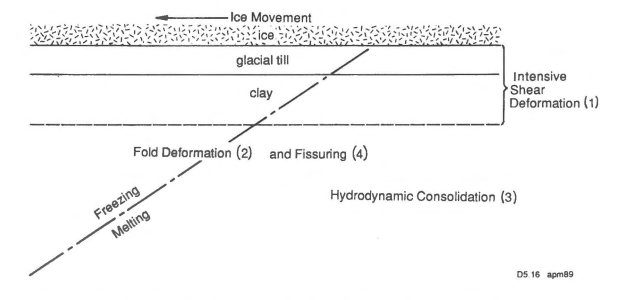


Fig. 7. Schematic diagram of sub-glacial deformation model.

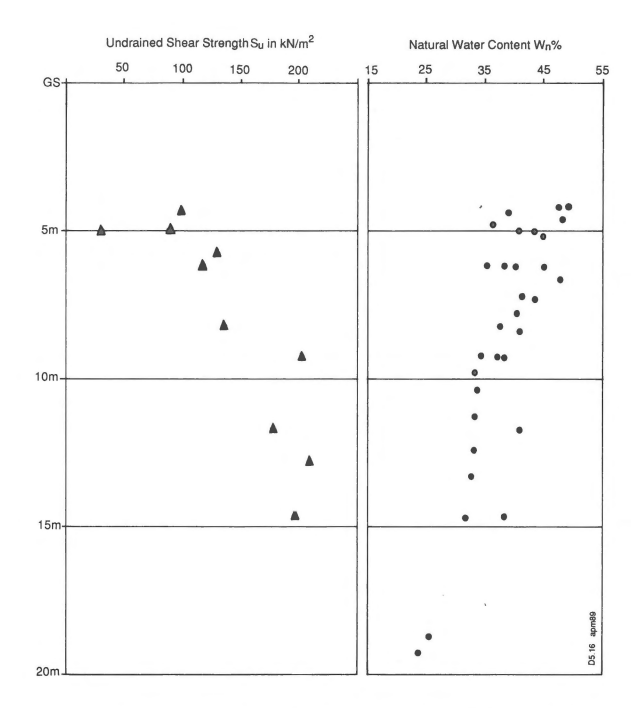


Fig. 8. Variation with depth of undrained shear strength  $(s_u)$  and natural moisture content  $(w_N)$  in Pot Clay in the area between Marum and Delfzijl.

dation tests (Fig. 9) are much higher then present in-situ stresses and show the overconsolidation of the Pot Clay. After gradual thawing of the subglacial sediments the Pot Clay could consolidate under the effective stresses which prevailed during the steady state phase of the ice sheet.

Meltwater production must have been such that a pore water pressure gradient could build up and be maintained during the steady state of the ice sheet, causing effective pressures to increase with depth (Fig. 9). This trend is also well shown by the geophysical spontaneous potential log, which is related to the density of the clay (Fig. 3).

The meaning of the measured maximum paleoeffective stress of 2100 kN/m<sup>2</sup> in terms of thickness of the ice sheet will be discussed in a forthcoming article (Schokking, 1990, this issue).

It can be concluded from the formation of pressure shadows of consolidated clay around folded silt bands (Fig. 12) that the consolidation occurred during or after the folding phase of (2).

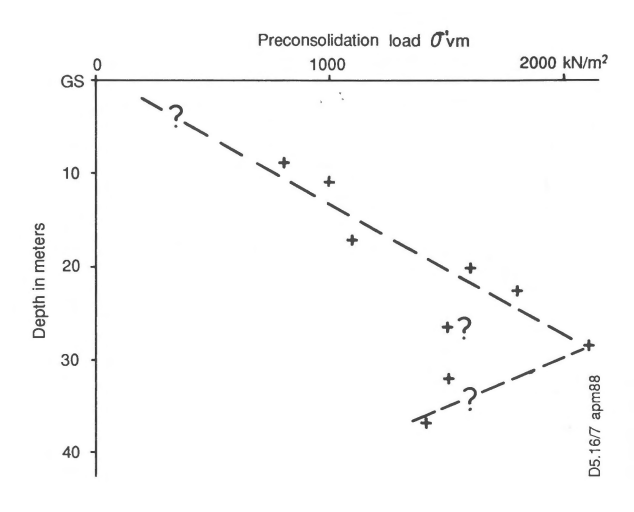


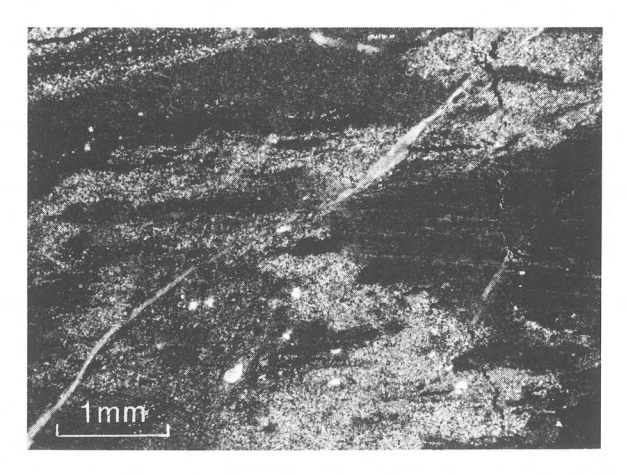
Fig. 9. Estimated preconsolidation loads vs. depth.

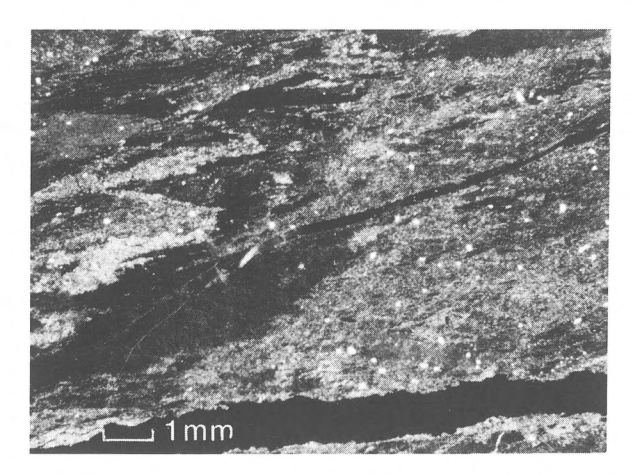
## (4) Fissuring

The homogeneous Pot Clay in the Marum borehole is crumbly and falls apart into small angular fragments when samples of the higher parts of the profile are broken. This characteristic appears to be mainly related to fissures, which can be observed in the halved samples (Figs 4, 5 & 13). The fissures are in general flat or slightly undulating and their surfaces show polished slickensides. SEM images of the fissures show that the clay particles have a strong preferred orientation parallel to the fissures (Fig. 14). Down to a depth of approximately 23 m the fissures are continuous through the diameter of the samples, they do, however, not continue in the sandy layers. Displacements along the fissures can not be seen with the naked eye, but thin sections reveal displacements in the order of 1 mm or less.

Within the same sample, the fissures have in general a preferred orientation, although opposite and vertical orientations also occur. In Fig. 13 the change in orientation with depth and in the spacing of the fissures are indicated. Although no oriented samples were taken, a relationship between the dip of the fissures and depth can be observed. Below 23 m the fissures become more discontinuous, less abundant and, at depth, attenuate to minor distortions in the clay.

The presence of the fissures can also be conclud-





Figs 10 and 11. Microfolding of silt lamination in clay. Note the diamond shaped clay packages and segregation structures in Fig. 10. Photograph with crossed polarizers.

ed from the undrained shear strength (s<sub>u</sub>) measurements (Fig. 6). These measurements were performed with two different methods on the same sample, the laboratory vane test using a 12.7 mm (height and diameter) vane and the Geonor fall cone test (as described by Hansbø 1957).

From the base of the sandy clay at  $10\,\mathrm{m}$  to  $25\,\mathrm{m}$  two ranges of  $s_\mathrm{u}$  values are measured,  $150\,\mathrm{to}$   $250\,\mathrm{kN/m^2}$  for the laboratory vane and  $250\,\mathrm{to}$   $400\,\mathrm{kN/m^2}$  for the fall cone. Although the values produced by both methods are disputable in various respects, their differences give an indication for the presence of fissures: the shear strength of the failure cylinder of the laboratory vane will in many cases be influenced by the fissures whereas, in the fall cone test, the strength of the clay material itself is tested; below  $25\,\mathrm{m}$ , in the zone where the fissures almost disappear,  $s_\mathrm{u}$ -values tend to coincide.

Figure 12, a photography of a thin section, indicates that the fissures cut across features that developed during deformation phases of (2) and (3), which supports the sequence of events described.

The development of the fissures in the clay, which was stiffend during phase (3), is explained to have been caused by the thrusting force of the ice. For the transmission of the thrusting force from the ice to the sub-glacial sediments one can think of several possibilities. In case the subsoil was unfrozen one has to accept the presence of a fast deforming, low strength, low density horizon, with

low effective stresses. The stresses thus transmitted, will only have been small, and although long term creep will have been involved in the deformation, it is unlikely, that such deep fissures would have developed in the very stiff clay.

An argument which favours a different interpretation, is that the clay layers between the sandy layers in the upper part of the sequence, which have a low undrained shear strength, a high moisture content, and have been subjected to relatively low effective stresses, do not show these predominantly parallel fissures. Instead the clay in this zone exhibits a random poligonal fissure pattern, which is interpreted to be the result of segregation by freezing.

It is more likely that the low density horizon was absent during some period as a result of changed thermal conditions. Without that horizon the stresses developed by a thrust force on the clay have then been equal to the shear strength within the ice mass.

That the fissures begin just at the base of the sandy layers may be due to changed strength conditions in case a continuous frozen clay body is assumed. A change in thermal conditions thanks to a difference in thermal conductivity may have been a contributing factor. The decrease in abundance of fissures with depth, can be explained partly by increased consolidation and hence strength of the clay. Besides that, the horizontal thrust force will

have diminished with depth, proportional to the part taken up as strain in the clay body. This last effect, combined with the increased effective stress and stiffness of the clay with depth, may explain the steeper dip of the fissures near the base of the clay sequence.

This sub-glacial deformation model implies that permafrost conditions prevailed during the advance and the retreat of the ice sheet, and that a steady state condition existed, during which the groundwater was mobile.

Geological evidence for such conditions during the Saalian glaciation has been given by several authors. From the absence of abundant glacio-fluvial sediments under the Saale glacial till Ter Wee (1983a) infers that the ice must have moved over frozen ground, under low temperature conditions, which did not allow the formation of significant meltwater deposits. Strunk (1983) and Nekrasov (1983) describe permafrost features which were present down to considerable depth during the Saalian glaciation, i.e., 13 m in the German Ruhr area and 130 m in Eastern Europe. This indicates, that permafrost occurred to significant depths in the northern Netherlands before and during the ice advance. During the advance of the ice sheet, the active layer developed each summer and played an important role in forming a volume of unfrozen soil over which movement of the ice sheet was possible. Thus conditions were created gouverned by high porewater pressures, low effective stresses and resulting low soil strength.

#### **Conclusions**

From the geotechnical, structural and microstructural properties of a 40 m thick Pot Clay sequence a sub-glacial deformation model connected to an ice sheet during the Saalian glaciation is constructed. Intense shear in a low density, low strength upper horizon, folding of the clay at natural water contents in a frozen or unfrozen state, hydrodynamic consolidation and the formation of fissures in the stiffened clay in the underlying sequence could be demonstrated. The low density upper zone has been observed to occur over a wide region.



Fig. 12. Microfolding of silt lamination in clay (29.5 m) showing pressure shadows of consolidated clay around it and crosscutting fissures. Photograph with crossed polarizers.

In the underlying horizon preconsolidation loads increase with depth, due to a steep paleo-pore water gradient, the result of melting at the base of the ice sheet. A maximum preconsolidation load of  $2100 \, \mathrm{kN/m^2}$  has been estimated.

The fissures steepen with depth and become less abundant below 23 m.

The sub-glacial sediment deformation model is based on structural phenomena produced by a very complex system of interactively operating glacial processes. As yet the model can only be described in rather broad terms. For a more advanced model more geotechnical and structural information is needed. Furthermore a study of the physical processes involved coupled to a parallel modelling thereof is required. Such modelling should take into account thermo-mechanically coupled ice flow, sub-glacial sediment deformation, sub-soil

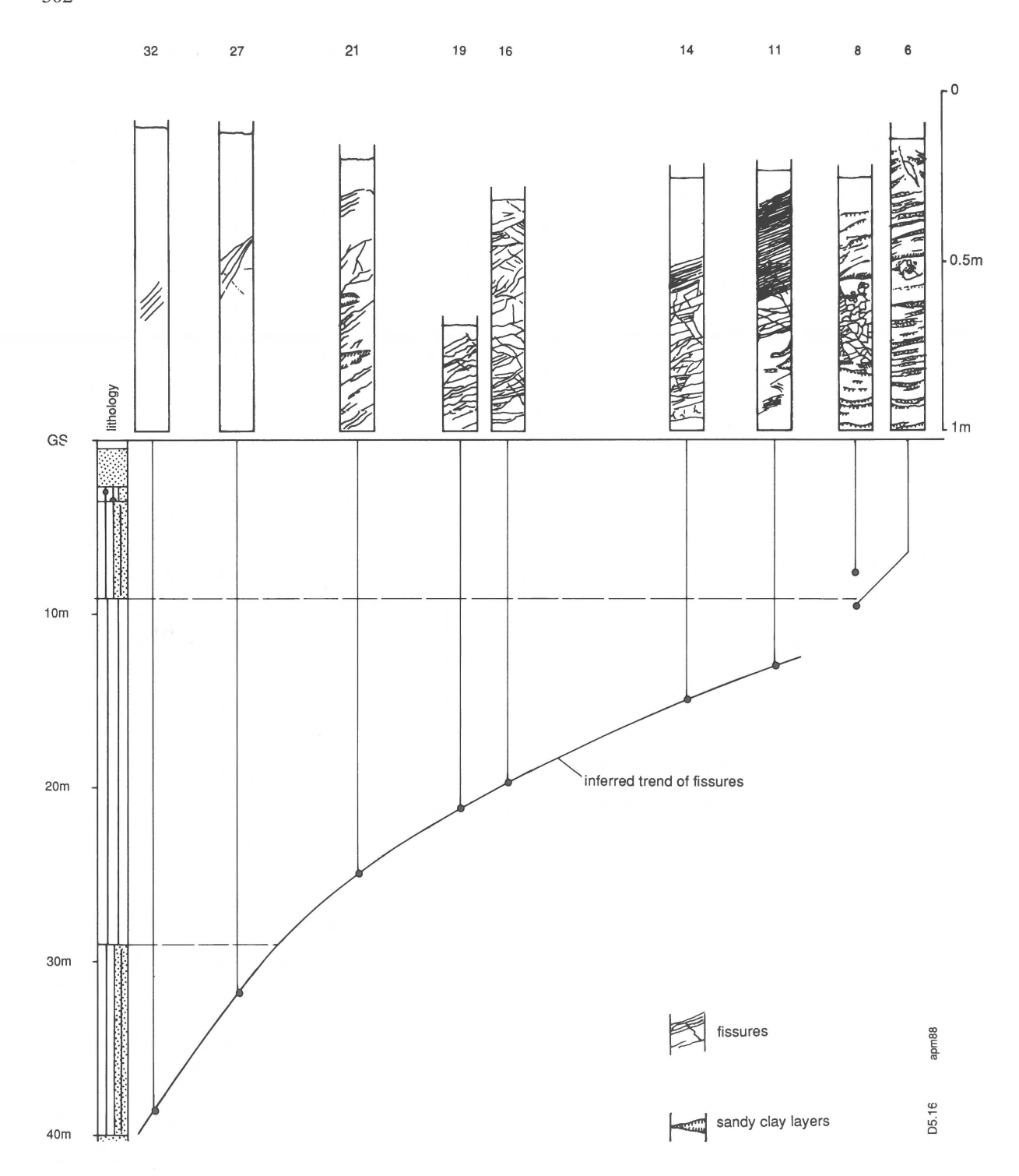


Fig. 13. Deformation and fissure pattern in opened samples and inferred trend of fissures.

temperature development and sub-glacial groundwater flow. At present such a modelling effort is undertaken by the Geology Department of Edinburgh University jointly with the author.

In its turn a sub-glacial model has applications for the development of a geotechnical model of the overridden sediments. For the design of geotechnical constructions on or in the Pot Clay one will have to know the distribution of parameters as moisture content, density, strength, elastic and consolidation properties.

The strength and consolidation properties appear to be strongly related to the distribution of sub-glacial paleo-effective stresses and the presence of fissures.

Material properties, such as moisture content, unit weight and strength of the clay material itself, depend on the effective stresses resulting from the combination of the ice load and the prevailing pore water pressures.

Mass properties of a larger volume of clay, such as strength, are influenced by the occurrence of fissures. This was demonstrated with differences in undrained shear strength values obtained with the laboratory vane and the cone test.

To obtain more information which can serve as a feedback for the glacial process modelling, but also to obtain more data on the geotechnical properties

Table 1. Glossary of geotechnical terms used

Term	Symbol	Unit
Natural Moisture Content	$\mathbf{w}_{\mathrm{L}}$	wt water wt solid · 100%
Plasticity or Atterberg Limits		
Liquid Limit	$\mathbf{w}_{\mathtt{L}}$	,,
Plastic Limit	$W_P$	,,
Plasticity Index	$w_L$ – $w_P$	,,
Saturated Unit Weight	$\gamma_s$	$kN/m^3$
Undrained Shear Strength	$S_u$	$kN/m^2$
Total Stress	$\sigma_{\rm v}$	,,
Water Pressure	u	,,
Effective Stress	$\sigma_{\rm v}{}' = \sigma_{\rm v} - u$	"
Increase in Total Stress	$\triangle \sigma_v$	,,
Increase in Water Pressure	△ u	,,
Increase in Effective Stress	$\triangle$ $\sigma_{v}{'}$	**
Preconsolidation Load	$\sigma_{vm}{}'$	"

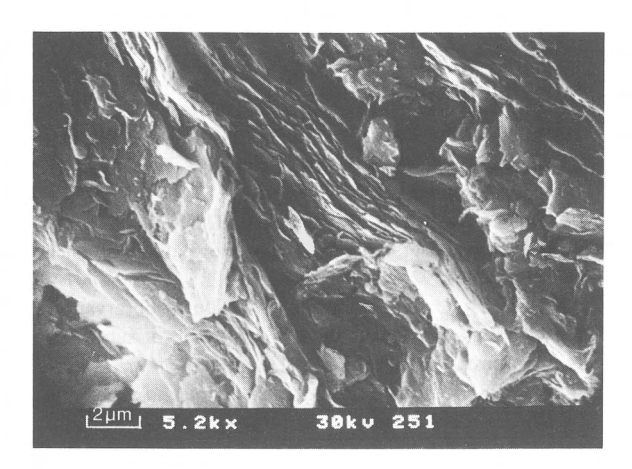


Fig. 14. SEM image of fissure in Pot Clay at 24.5 m. Before exposure sample coated with evaporated gold. Image obtained with ISI SS 40 SEM, with secondary electron detector.

of the Pot Clay further research is presently carried out at other locations in the region.

## Acknowledgements

I thank Prof. G.S. Boulton of Edinburgh University and D.J. Beets of the Geological Survey of The Netherlands for helpful discussions and Prof. D.C. Price of the Technical University Delft for critically reading the article.

Thanks also to my colleagues of the Geological Survey of The Netherlands, H. Poortinga and C. van der Meulen for drilling the borehole, P. Zonneveld who took care of the geotechnical laboratory testing and P. Marselje for drawing services.

Finally thanks to Mr. Lam Sia Keng, Engineering Geologist of the Geological Survey of Malaysia, Kuching, Sarawak Branch, who assisted with the geotechnical testing, during his training at the Geological Survey.

#### **Notes**

- 1. A glossary of geotechnical terms and symbols is given in Table 1.
- 2. All depths mentioned in this paper refer to levels below ground surface, unless indicated otherwise.

#### References

- Bisdom, E.B.A. 1987 Toepassing van een internationaal micromorfologisch beschrijvingssysteem op tien grote slijpplaten van kleimonsters uit Nederland en België – Rep. STIBOKA Nr. 1850, Wageningen, 1987: 56 pp
- Boulton, G.S. & R.C.A. Hindmarsh 1987 Sediment deformation beneath glaciers: rheology and geological consequences— J. Geoph. Res. 92, (B9), 9059–82: 1–39
- Echelmeyer, K. & W. Zhongxiang 1987 Direct observation of basal sliding and deformation of basal drift at sub-freezing temperatures J. Glaciol, 33, 113: 83–98
- Ehlers, J. 1981 Some aspects of glacial erosion and deposition in North Germany – Ann. of Glaciol 2: 143–146
- Hansbø, S. 1957 A new approach to the determination of the shear strength of clay by the fall-cone test Swed. Geotech. Inst., Proc. 14
- Jongerius, A. & G. Heintzberger 1975 Methods in soil micromorphology. A technique for the preparation of large thin sections Neth. Soil Surv. Inst., Wageningen, Soil Surv. Pap. 10: 48 pp.
- Nekrasov, I.A. 1983 Dynamics of the cryolithozone in the northern hemisphere during the Pleistocene. In: Proc. 4th Int. Conf. Permafrost, 1983, Fairbanks, Alaska, U.S.A.: 903–906

- Savigny, K.W. & N.R. Morgenstern 1986 Creep behaviour of undisturbed clay permafrost – Can. Geotech. J. 23: 515–527
- Schokking, F. 1984 Inventarisatie van slecht-doorlatende laagpakketten in de ondergrond van het Nederlandse vasteland – Rept. Rijks Geol. Dienst, OP 6009, Haarlem: 131 pp
- Schokking, F. 1985 Onderzoek naar geschikte locatie voor offshore paaltest in Oost-Groningen – Rept. Rijks Geol. Dienst, BP 10565, Haarlem: 7 pp
- Strunk, H. 1983 Pleistocene diapiric upturnings of lignites and clayey sediments as periglacial phenomena in Central Europe. In: Proc. 4th Int. Conf. Permafrost, 1983, Fairbanks, Alaska, U.S.A.: 1200–1204
- Schokking, F. 1990 On estimating the thickness of the Saalian ice sheet from a vertical profile of preconsolidation loads of a lacustro-glacial clay Geol. Mijnbouw 69: 291–304 (this issue)
- Ter Wee, M.W. 1983a The Saalian glaciation in the northern Netherlands. In: Ehlers, J. (ed.): Glacial deposits in North-West Europe – Balkema: 405–412
- Ter Wee, M.W. 1983b The Elsterian Glaciation in The Netherlands. In: Ehlers, J. (ed.): Glacial deposits in North-West Europe Balkema: 413–415
- Van den Berg, M.W. & J.D. Beets 1986 Saalian glacial deposits and morphology in The Netherlands. In: Van der Meer, J.J.M. (ed.): Proc. of INQUA Symp. on the Genesis and Lithology of Glacial Deposits – Balkema: 270 pp